

Isomer Distribution and Interconversion in Cationic Allylpalladium(II) Complexes with 2-(Iminomethyl)pyridine Ligands

Bruno Crociani,* Simonetta Antonaroli, and Maurizio Paci

Dipartimento di Scienze e Tecnologie Chimiche, Università di Roma "Tor Vergata",
00133 Rome, Italy

Francesca Di Bianca

Dipartimento di Chimica Inorganica, Università di Palermo, Palermo, Italy

Luciano Canovese

Dipartimento di Chimica, Università di Venezia, Venice, Italy

Received October 2, 1996[®]

The complexes $[\text{Pd}(\eta^3\text{-allyl})(\text{N-N}')]\text{ClO}_4$ [allyl = 2-butenyl or 3-methyl-2-butenyl, N-N' = $\text{C}_5\text{H}_3(6\text{-R})\text{N-2-CH=NR}'$ (R = H, R' = Me, CMe_3 , $\text{C}_6\text{H}_4\text{OMe-4}$; R = Me, R' = $\text{C}_6\text{H}_4\text{OMe-4}$) and $\text{C}_5\text{H}_4\text{N-2-CH}_2\text{NMe}_2$] are present in solution with different isomers, the structures of which may be assigned by an ^1H NMR criterion based on chemical shift changes of the pyridine H(6) and/or of the allylic methyl protons, as confirmed also by 2D ^1H NMR spectra. The isomer distribution depends mainly on the steric requirements of both the allyl and N-N' ligands: for $[\text{Pd}(\eta^3\text{-3-methyl-2-butenyl})(\text{N-N}')]\text{ClO}_4$ the predominant isomer (ca. 100%) has a structure with the allylic methyl groups *cis* to the coordinated pyridine nitrogen when N-N' = $\text{C}_5\text{H}_4\text{N-2-CH=NCMe}_3$ and *cis* to the coordinated imino nitrogen when N-N' = $\text{C}_5\text{H}_3(6\text{-Me})\text{N-2-CH=NC}_6\text{H}_4\text{OMe-4}$. In chlorinated solvents (dichloromethane- d_2 or 1,1,2,2-tetrachloroethane- d_2) the isomers undergo mutual interconversion through a mechanism involving an apparent rotation of the η^3 -allyl ligand around its bond axis to the metal. The interconversion rates depend on the nature of allyl and N-N' ligands and increase considerably when the compounds are dissolved in dimethyl- d_6 sulfoxide. The apparent allyl rotation also occurs for the analogous (η^3 -2-methyl-2-propenyl)palladium(II) derivatives. For $[\text{Pd}(\eta^3\text{-2-methyl-2-propenyl})(\text{N-N}')]\text{ClO}_4$ [N-N' = $\text{C}_5\text{H}_3(6\text{-Me})\text{N-2-CH=NC}_6\text{H}_4\text{OMe-4}$] the allyl rotation rate increases with increasing concentration up to a limiting constant value. This behavior is interpreted on the basis of a mechanism involving a fast and reversible association of the cationic complex with the perchlorate anion to form a loose ion pair which undergoes a rate-determining molecular geometry rearrangement upon coordination of ClO_4^- . For a solution of $[\text{Pd}(\eta^3\text{-3-methyl-2-butenyl})(\text{N-N}')]\text{ClO}_4$ (N-N' = $\text{C}_5\text{H}_4\text{N-2-CH}_2\text{NMe}_2$) in 1,1,2,2-tetrachloroethane- d_2 , the 2-D ROESY spectrum suggests that the apparent allyl rotation at 28 °C does not involve Pd–NMe₂ bond breaking. The rupture of this bond takes place when the temperature is raised to ca. 90 °C or when the complex is dissolved in dimethyl- d_6 sulfoxide at ambient temperature.

Introduction

Palladium-catalyzed nucleophilic substitution on allylic substrates is an important and versatile reaction which has attracted a great deal of interest for its potential synthetic applications.¹ The accepted mechanism involves an oxidative addition of the allylic substrate to a palladium(0) species to form an (η^3 -allyl)-palladium(II) intermediate, which is subsequently attacked by the incoming nucleophile to yield the substi-

tuted allylic product and regenerate the initial palladium(0) complex. With the so-called "soft" nucleophiles (amines and carbon nucleophiles with $\text{p}K_{\text{a}} < 20$) the attack generally occurs at a terminal carbon atom of the η^3 -bound allyl group on the face opposite to the metal center.

Despite the large number of studies, the general problem of steric and/or electronic control of the regio- and enantioselectivity has yet to be solved, one of the main difficulties being the large distance between a palladium-coordinated chiral ligand and the site of the nucleophilic attack.² In some cases, asymmetric syntheses with high ee have been obtained by using bulky chiral ligand of propeller type or of C_2 symmetry.³ In

[®] Abstract published in *Advance ACS Abstracts*, January 1, 1997.

(1) (a) Trost, B. M.; Verhoeven, T. R. In *Comprehensive Organometallic Chemistry*; Wilkinson, G., Stone, F. G. A., Abel, E. W., Eds.; Pergamon Press: Oxford, U.K., 1982; Vol. 8, Chapter 57. (b) Godleski, S. A. In *Comprehensive Organic Synthesis*; Trost, B. M., Fleming, I., Eds.; Pergamon Press: Oxford, U.K., 1991; Vol. 4, Chapter 3.3. (c) Hegedus, L. S. In *Organometallics in Synthesis*; Schlosser, M., Ed.; John Wiley and Sons: Chichester, U.K., 1994; Chapter 5.4.3. (d) Tsuji, J. *Palladium Reagents and Catalysts*; John Wiley and Sons: Chichester, U.K., 1995; Chapter 4.2.

(2) (a) Frost, C. G.; Howarth, J.; Williams, J. M. J. *Tetrahedron Asym.* **1992**, *3*, 1089. (b) Noyori, R. *Asymmetric Catalysis In Organic Synthesis*; John Wiley and Sons, Inc.: New York, 1994; Chapter 4. (c) Reiser, O. *Angew. Chem., Int. Ed. Engl.* **1993**, *32*, 547.

other cases, a high degree of enantioselectivity has been achieved by exploiting the combined steric and electronic properties of chiral bidentate asymmetric ligands with a set of ligating atoms of the same or different nature.⁴

The ligand-induced control, however, depends on the relative rates of nucleophilic substitution at the allyl group and the dynamic processes of the (η^3 -allyl)-palladium(II) intermediates, which may rearrange into various enantio- or diastereomeric forms through different mechanisms, such as the allylic η^3 - η^1 - η^3 interconversion,^{4g,5} the redox allyl transfer from a palladium(II) to a palladium(0) center,⁶ and the apparent rotation of the η^3 -bound allyl group around its bond axis to the metal.^{5b,7} The latter process was studied mainly with cationic complexes $[\text{Pd}(\eta^3\text{-allyl})(\text{N-N}')^+]$ with bidentate nitrogen ligands N-N'. Two mechanisms have been proposed: a dissociative mechanism involving three-coordinate T-shaped intermediates^{7b,c} and an associative mechanism involving stereochemically nonrigid five-coordinated intermediates.^{5b,7a} The dissociative mechanism is supported by the ¹H NMR observation of Pd-N bond rupture in the dynamic behavior of $[\text{Pd}(\eta^3\text{-allyl})(\text{bpm})]^+$ complexes containing asymmetrically substituted allyl groups and the 2,2'-bipyrimidine ligand (bpm).^{7c} The associative mechanism is supported by the accelerating effect on the rate of apparent rotation upon addition of neutral or anionic ligands, such as free N-N' or Cl⁻,^{7a} and by the negative entropy of activation measured for this process.^{5b}

Due to our interest in this area, we report herein the results of a ¹H NMR study on the isomer distribution and the mechanism of isomer interconversion for the complexes $[\text{Pd}(\eta^3\text{-allyl})(\text{N-N}')\text{ClO}_4]$ reported in Scheme 1.

(3) (a) Trost, B. M.; Van Vranken, D. L.; Bingle, C. *J. Am. Chem. Soc.* **1992**, *114*, 9327. (b) Leutenegger, U.; Umbricht, G.; Fahrni, C.; von Matt, P.; Pfaltz, A. *Tetrahedron* **1992**, *48*, 2143. (c) Kubota, H.; Nakajima, M.; Koga, K. *Tetrahedron Lett.* **1993**, *34*, 8135. (d) Bovens, M.; Togni, A.; Venanzi, L. M. *J. Organomet. Chem.* **1993**, *451*, C28. (e) Pregosin, P. S.; Rügger, H.; Salzmänn, R.; Albinati, A.; Lianza, F. *Organometallics* **1994**, *13*, 83. (f) Tarmer, D.; Anderson, P. G.; Harden, A.; Somfasi, P. *Tetrahedron Lett.* **1994**, *35*, 4631. (g) Gamez, P.; Dunjic, B.; Fache, F.; Lemaire, M. *J. Chem. Soc., Chem. Commun.* **1994**, 1417. (h) Legros, J. T.; Fiaud, J. C. *Tetrahedron* **1994**, *50*, 465. (i) Trost, B. M.; Richard, C. B. *J. Am. Chem. Soc.* **1994**, 4089. (j) Trost, B. M.; Breit, B.; Organ, M. G. *Tetrahedron Lett.* **1994**, 5817. (k) Trost, B. M.; Lee, C. B.; Weiss, J. M. *J. Am. Chem. Soc.* **1995**, *117*, 7247. (l) Trost, B. M.; Organ, M. G.; O'Doherty, G. A. *J. Am. Chem. Soc.* **1995**, *117*, 9662.

(4) (a) Sawamura, M.; Nagota, H.; Sakamoto, H.; Ito, Y. *J. Am. Chem. Soc.* **1992**, *114*, 2586. (b) Sprinz, J.; Helmchen, G. *Tetrahedron Lett.* **1993**, *34*, 1769. (c) von Matt, P.; Pfaltz, A. *Angew. Chem., Int. Ed. Engl.* **1993**, *32*, 566. (d) Kubota, H.; Koga, K. *Tetrahedron Lett.* **1994**, *35*, 6689. (e) Frost, C. G.; Williams, J. M. J. *Synlett.* **1994**, 551. (f) Allen, J. V.; Coote, S. J.; Dawson, G. J.; Frost, C. G.; Martin, C. J.; Williams, J. M. J. *J. Chem. Soc., Perkin Trans. 1* **1994**, 2065. (g) Sprinz, J.; Kiefer, M.; Helmchen, G.; Reggelin, M.; Huttner, G.; Walter, O.; Zsolnai, O. W. *Tetrahedron Lett.* **1994**, *35*, 1523. (h) Togni, A.; Venanzi, L. M. *Angew. Chem., Int. Ed. Engl.* **1994**, *33*, 497. (i) Abbenhuis, H. C. L.; Burckhardt, U.; Gramlich, V.; Koellner, K.; Pregosin, P. S.; Salzmänn, R.; Togni, A. *Organometallics* **1995**, *14*, 759.

(5) (a) Cesarotti, E.; Grassi, M.; Prati, L.; Demartin, F. *J. Organomet. Chem.* **1993**, *12*, 4940. (b) Hansson, S.; Norrby, P. O.; Sjögren, M. P. T.; Akermarck, B.; Cucciolito, M. E.; Giordano, F.; Vitagliano, A. *Organometallics* **1993**, *12*, 4940. (c) Gatti, G.; López, J. A.; Mealli, C.; Musco, A. *J. Organomet. Chem.* **1994**, *483*, 77. (d) Breutel, C.; Pregosin, P. S.; Salzmänn, R.; Togni, A. *J. Am. Chem. Soc.* **1994**, *116*, 4067. (e) Pregosin, P. S.; Salzmänn, R.; Togni, A. *Organometallics* **1995**, *14*, 842. (f) Barbaro, P.; Pregosin, P. S.; Salzmänn, R.; Albinati, A.; Kunz, R. W. *Organometallics* **1995**, *14*, 5160.

(6) (a) Granberg, K. L.; Bäckvall, J. E. *J. Am. Chem. Soc.* **1992**, *114*, 6858. (b) Ogoshi, S.; Kurosawa, H. *Organometallics* **1993**, *12*, 2869.

(7) (a) Crociani, B.; Di Bianca, F.; Giovenco, A.; Boschi, T. *Inorg. Chim. Acta* **1987**, *127*, 169. (b) Albinati, A.; Kunz, K. W.; Ammann, C. J.; Pregosin, P. S. *Organometallics* **1991**, *10*, 1800. (c) Gogoll, A.; Örnebro, J.; Grennberg, H.; Bäckvall, J. E. *J. Am. Chem. Soc.* **1994**, *116*, 3631.

Scheme 1

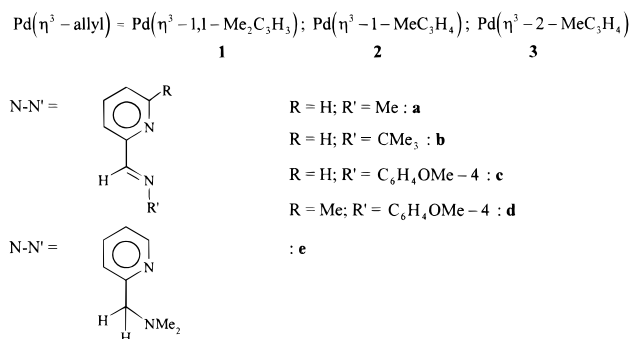


Chart 1

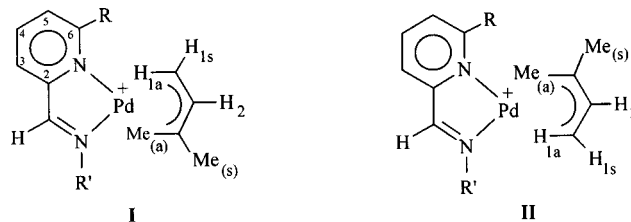
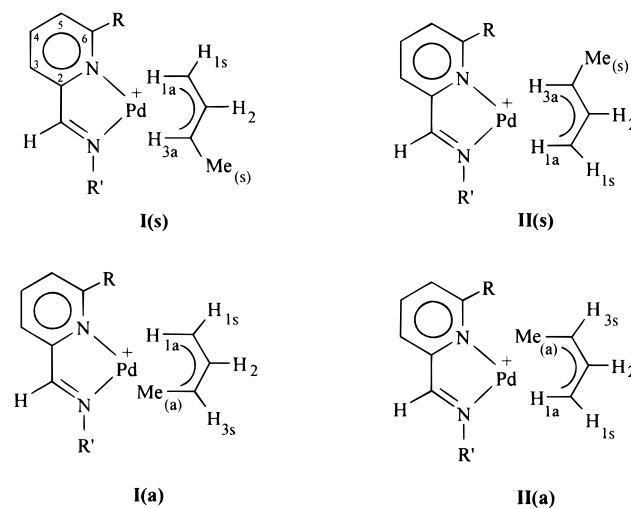


Chart 2



Results and Discussion

Isomer Distribution. The cationic complexes $[\text{Pd}(\eta^3\text{-allyl})(\text{N-N}')^+]$ containing asymmetric N-N' ligands and asymmetrically substituted allyl groups may be present in solution with various isomers. The number of the possible isomers ranges from 2 for the η^3 -3-methyl-2-butenyl derivatives **1a-e** (Chart 1) to 4 for the η^3 -2-butenyl derivatives **2a-e**, due to the allylic *syn* and *anti* configurations in the latter compounds (Chart 2).

In any case, each isomer is accompanied by its enantiomeric form, which cannot be directly distinguished in the ¹H NMR spectra, under the experimental conditions used in this study. On the other hand, the isomers of structure **I** and **II** undergo mutual exchange in solution with interconversion rates which may be high (on the NMR time scale) at ambient temperature as to give rise to time-averaged proton NMR resonances. Upon cooling of the solution, however, the different isomers are easily detected by ¹H NMR spectroscopy, as is shown in Figure 1 for the complex **1c**(ClO₄). As can be seen, the main spectral differences are found for the pyridine H(6) and for the allyl H_{1s} resonances, which

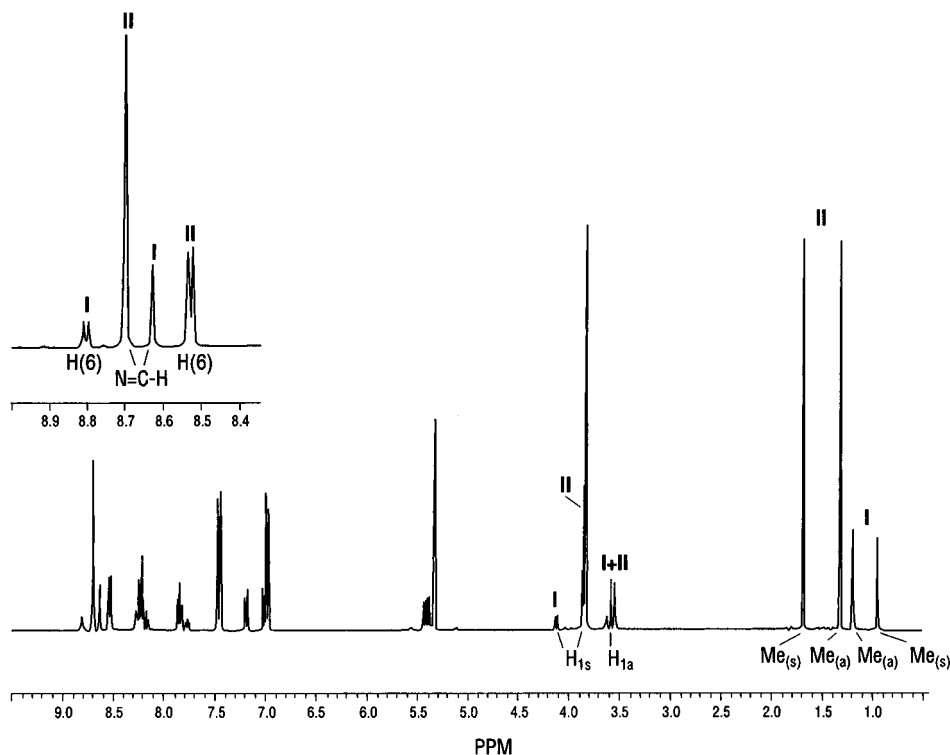


Figure 1. ^1H NMR spectrum of complex **1c**(ClO_4) in dichloromethane- d_2 at -60°C . The inset shows in detail the enlarged range 9.0–8.4 ppm.

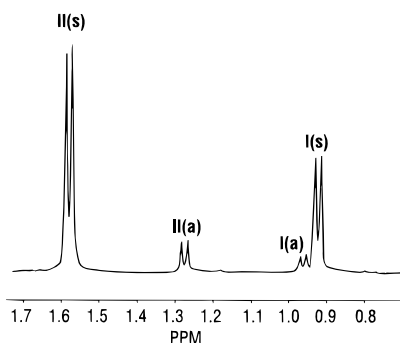


Figure 2. ^1H NMR spectrum of complex **2c**(ClO_4) in dichloromethane- d_2 at -60°C in the range 1.7–0.8 ppm.

are shifted upfield of *ca.* 0.3 ppm in the major isomer **II**, and for both the allyl $\text{Me}_{(s)}$ and $\text{Me}_{(a)}$ resonances, which occur at remarkably higher field in the minor isomer **I**.

The shieldings of the H_{1s} proton in **II** and of the $\text{Me}_{(s)}$ and $\text{Me}_{(a)}$ protons in **I** are clearly due to the anisotropic effect of the aromatic $\text{C}_6\text{H}_4\text{OMe-4}$ imino substituent in **1c**, since they are not observed for the isomers of the corresponding complex **1a**(ClO_4) where the imino substituent is a methyl group. For the isomers of **1a**, however, a difference of 0.26 ppm in the chemical shift of H(6) is still present (see Table 1).

The influence of the imino $\text{C}_6\text{H}_4\text{OMe-4}$ substituent in **1c** may be rationalized in terms of shielding effects of the aromatic ring currents, which bring about an upfield shift for the H_{1s} signal in a structure of type **II** for the major isomer [where the allyl H_{1s} proton is on the same side (*cis* position) relative to $\text{R}' = \text{C}_6\text{H}_4\text{OMe-4}$] and for the $\text{Me}_{(s)}$ and $\text{Me}_{(a)}$ signals in a structure of type **I** for the minor isomer (where the allyl methyl groups are on the same side relative to $\text{R}' = \text{C}_6\text{H}_4\text{OMe-4}$) if the

phenyl ring of the $\text{C}_6\text{H}_4\text{OMe-4}$ moiety is noncoplanar with the palladium coordination plane. Similar anisotropic shieldings arising from noncoplanarity of aromatic *N*-imino substituents with the metal coordination plane have been observed in complexes $[\text{Pd}(\text{N}-\text{N}')(\eta^2\text{-dmf})]$ [$\text{N}-\text{N}' = \text{bis}(\text{arylimino})\text{acenaphthene}$; *dmf* = dimethyl fumarate].⁸ The upfield shift of the pyridine H(6) resonance of the *N*-*N'* ligands with $\text{R} = \text{H}$ on going from structure **I** to structure **II**, in which the H(6) proton is *cis* to the allylic $\text{Me}_{(s)}$ group, and the upfield shifts of both the $\text{Me}_{(s)}$ and $\text{Me}_{(a)}$ resonances on going from structure **II** to structure **I**, in which the allylic $\text{Me}_{(s)}$ and $\text{Me}_{(a)}$ groups are *cis* to $\text{R}' = \text{C}_6\text{H}_4\text{OMe-4}$, appear to be quite general in the ^1H NMR spectra of the η^3 -3-methyl-2-butenyl complexes as well as in those of the η^2 -2-butenyl analogs (Table 2). These shifts, therefore, can be taken as diagnostic for assigning the isomer structures in solution.

It is noteworthy that the *syn* Me protons of **2c** undergo a much larger shielding ($\Delta\delta$ 0.66 ppm), when the structure is changed from **II**(**s**) to **I**(**s**), than the *anti* Me protons ($\Delta\delta$ 0.31 ppm), when the structure is changed from **II**(**a**) to **I**(**a**), as shown in Figure 2. This effect occurs also in the isomers **I** and **II** of the η^3 -3-methyl-2-butenyl complexes **1c,d** to such extent as to invert the chemical shift sequence of $\text{Me}_{(s)}$ and $\text{Me}_{(a)}$ protons. As will be discussed later, in the isomer **II** of **1d** the $\text{Me}_{(s)}$ resonance is found at higher field (0.64 ppm) relative to that of the $\text{Me}_{(a)}$ protons (1.14 ppm), in contrast to the usual trend of allylic systems in which the *anti* protons generally resonate at higher field.

The structure assignment, based on chemical shift changes of pyridine H(6) and/or allyl $\text{Me}_{(s)}$ and $\text{Me}_{(a)}$ protons for the isomers of the cationic complexes **1a–e**

(8) van Asselt, R.; Elsevier, C. J.; Smeets, W. J. J.; Spek, A. L. *Inorg. Chem.* **1994**, *33*, 1521.

Table 1. ^1H NMR Data^a for the Complexes **1a–e**(ClO₄)

complex	isomer distributn ^b	allyl protons ^c				N–N' protons ^d			other signals
		H _{1a}	H _{1s}	Me _(a)	Me _(s)	N=CH	H(6)	Me(6)	
1a	I (56%)	3.50 d (13.3)	4.04 d (7.5)	1.27 s	1.66 s	8.69 q (1.1) ^e	8.71 m		3.73 d [N–Me]
	II (44%)	3.41 d (13.6)	4.04 d (7.5)	1.27 s	1.68 s	8.61 q (1.2) ^e	8.45 m		3.86 d [N–Me]
1b	II (100%)	3.42 d (13.3)	4.25 d (7.2)	1.26 s	1.68 s	8.54 s	8.52 m		1.40 s [CMe ₃]
1c	I (21%)	3.59 d (13.0)	4.11 d (7.3)	1.18 s	0.94 s	8.62 s	8.80 m		
	II (79%)	3.55 d (13.4)	3.84 d (7.3)	1.31 s	1.69 s	8.70 s	8.52 m		
1d	I (100%)	3.38 d (13.1)	4.26 d (7.3)	1.14 s	0.64 s	8.58 s		2.75 s	
1e^f	I (47%)	3.36 d (13.0)	3.87 d (7.7)	1.23 s	1.49 s		8.52 m		2.72 s, 2.59 s [NMe ₂]
	II (53%)	3.31 d (13.0)	3.79 d (7.7)	1.26 s	1.58 s		8.30 m		2.82 s, 2.76 s [NMe ₂]

^a In dichloromethane-*d*₂ at –60 °C, unless otherwise stated; s = singlet, d = doublet, dd = doublet of doublets, q = quartet, m = multiplet, mk = masked. ^b From integration data. ^c Numbering of allylic protons as in Chart 1; coupling constants with the central H₂ proton in parentheses. ^d Numbering of pyridine protons as in Chart 1. ^e Coupling constants with the N–Me protons. ^f In 1,1,2,2-tetrachloroethane-*d*₂ at 28 °C.

Table 2. ^1H NMR Data^a for the Complexes **2a–e**(ClO₄)

complex	isomer distributn ^b	allyl protons ^c				N–N' protons ^d			other signals
		H _{1a}	H _{3a}	H _{1s}	H _{3s}	Me	N=CH	H(6)	
2a	I(s) (52%)	3.28 d (12.4)	4.02 dq (11.9)	4.07 d (6.5)		1.56 d (5.9) ^e	8.70 q (1.0) ^f	8.68 m	3.73 d [N–Me]
	II(s) (40%)	3.19 d (12.3)	4.02 dq (11.9)	4.07 d (6.5)		1.58 d (5.8) ^e	8.64 q (1.2) ^f	8.44 m	3.86 d [N–Me]
	I(a) (4%)	3.52 d (13.4)		4.14 d (7.7)	4.95 dq (7.1)	1.20 d (6.8) ^e	8.61 q (1.3) ^f	mk	3.87 d [N–Me]
2b	II(a) (4%)	3.63 d (13.4)		4.19 d (7.6)	5.01 dq (7.1)	1.22 d (6.5) ^e	8.66 q (1.4) ^f	mk	
	I(s) (8%)	3.47 d (12.5)	mk	4.10 d (6.6)		mk	mk	8.76 m	
	II(s) (72%)	3.20 d (12.6)	4.15 dq (11.9)	4.32 d (6.6)		1.60 d (6.0) ^e	8.60 s	8.54 m	1.43 s [CMe ₃]
2c	I(a) (5%) ^g	3.76 d (13.2)		mk	mk	1.22 d (6.6) ^e	mk	mk	
	II(a) (15%) ^g	3.54 d (13.5)		mk	5.11 dq (6.9)	1.26 d (6.5) ^e	8.57 s	8.78 m	
	I(s) (30.5%)	3.51 d (12.5)	4.05 dq (11.7)	4.22 d (6.9)		0.92 d (6.2) ^e	8.68 s	8.76 m	
2d	II(s) (59%)	3.33 d (12.4)	4.13 dq (11.8)	3.80 ^h		1.58 d (6.2) ^e	8.72 s	8.51 m	
	I(a) (4%)	3.69 d (13.4)		4.23 ⁱ	4.83 dq (6.7)	0.96 d (7.1) ^e	mk	mk	
	II(a) (6.5%)	3.67 d (13.4)		3.98 d (7.5)	5.08 dq (6.8)	1.27 d (6.8) ^e	8.73 s	8.78 m	
2e^j	I(s) (78%)	3.30 d (12.6)	4.09 dq (11.6)	4.44 d (7.0)		0.63 d (6.2) ^e	8.61 s		2.71 s
	I(a) (16%)	3.48 d (13.4)		4.36 d (7.5)	4.70 dq (7.0)	0.89 d (6.7) ^e	8.64 s		2.73 s
	II(a) (6%)	3.67 d (13.4)		mk	mk	1.21 d (6.7) ^e	mk		2.78 s
2e^j	I(s) (38%)	3.18 d (11.6)	4.0–3.8 ^k	3.89 d (7.3)		1.41 d (6.2) ^e		8.50 m	2.82 s, 2.59 s [NMe ₂]
	II(s) (54%)	3.09 d (12.3)	4.0–3.8 ^k	3.80 d (7.0)		1.47 d (6.2) ^e		8.31 m	2.85 s, 2.75 s [NMe ₂]
	I(a) (4%)	3.45 d (12.1)		mk	4.77 dq (6.7)	1.20 d (6.7) ^e		8.53 m	
II(a) (4%)	3.45 d (12.1)		mk	4.62 dq (6.7)	1.17 d (6.7) ^e		8.53 m	2.90 s, 2.81 s, 2.79 s [NMe ₂]	

^a As footnote *a* of Table 1. ^b From integration data. ^c Numbering of allylic protons as in Chart 2; coupling constants with the central H₂ proton in parentheses. ^d Numbering of pyridine protons as in Chart 2. ^e Coupling constants ³J(HCC₃H₃). ^f Coupling constants with the N–Me protons. ^g Tentative assignment based on steric grounds. ^h Partially overlapping with the OMe signal. ⁱ Partially overlapping with the H_{1s} signal of isomer **I(s)**. ^j In 1,1,2,2-tetrachloroethane-*d*₂. ^k Overlapping signals.

Table 3. 2D ^1H NMR Data^a for the Complexes **1b**(ClO₄), **1d**(ClO₄), **1e**(ClO₄)^c

complex	interligand NOEs	selected intraligand NOEs
1b (isomer II)	H(6) [8.58]...Me _(s) [1.72] (s)	N=CH [8.60]...CMe ₃ [1.47] (s)
	H(6) [8.58]...Me _(a) [1.33] (w)	N=CH [8.60]...H(3) [8.15] ^d (s)
1d (isomer I)	CMe ₃ [1.47]...H _{1s} [4.29] (s)	H ₂ [5.38]...Me _(s) [1.72] (s)
	CMe ₃ [1.47]...H _{1a} [3.47] (s)	H _{1a} [3.47]...Me _(a) [1.33] (m)
	Me(6) [2.80]...H _{1s} [4.29] (w)	N=CH [8.62]...H(3) [7.95] ^d (s)
	Me(6) [2.80]...H _{1a} [3.44] (w)	Me(6) [2.80]...H(5) [7.70] ^e (s)
1e (isomer I)	H _(meta) [7.05] ^f ...Me _(a) [1.21] (m)	OMe [3.87]...H _(meta) [7.05] ^f (s)
	H(6) [8.52]...H _{1s} [3.87] (w)	H ₂ [5.25]...Me _(s) [0.78] (m)
	NMe ₂ [2.72]...Me _(a) [1.23] (m)	H _{1a} [3.44]...Me _(a) [1.21] (m)
1e (isomer II)		NCH ₂ [4.05]...H(3) [7.53] ^d (s)
		H ₂ [5.33]...Me _(s) [1.49] (s)
		H _{1a} [3.36]...Me _(a) [1.23] (m)
		NCH ₂ [4.05]...H(3) [7.53] ^d (s)
		H ₂ [5.33]...Me _(s) [1.58] (s)
		H _{1a} [3.31]...Me _(a) [1.26] (m)

^a Values in brackets are the proton chemical shifts in ppm; s = strong, m = medium, w = weak. ^b In dichloromethane-*d*₂ at 28 °C. ^c In 1,1,2,2-tetrachloroethane-*d*₂ at 28 °C. ^d H(3) proton on the pyridine ring. ^e H(5) proton on the pyridine ring. ^f H(3) and H(5) protons on the C₆H₄OMe-4 ring.

and **2a–e**, has been confirmed by 2D ^1H NMR ROESY experiments carried out on dichloromethane-*d*₂ solutions of **1b**(ClO₄) and **1d**(ClO₄) and on a 1,1,2,2-tetrachloroethane-*d*₂ solution of **1e**(ClO₄) at ambient temperature. The choice of these compounds stems from the fact that complexes **1b,d** are present in solution almost exclusively with a single isomer, namely isomer **II** for **1b** and isomer **I** for **1d**, whereas complex

1e exists as a mixture of isomers **I** and **II** in ca. 1:1.1 molar ratio. Some selected NOEs are reported in Table 3. The observed interligand NOEs between the η^3 -allyl and the chelating N–N' protons are in a complete agreement with the proposed structures. For instance, in the 2-D spectrum of **1b** the NOE cross-peak of the Me_(s) and Me_(a) protons with the H(6) pyridine proton and those of the H_{1s} and H_{1a} protons with the CMe₃

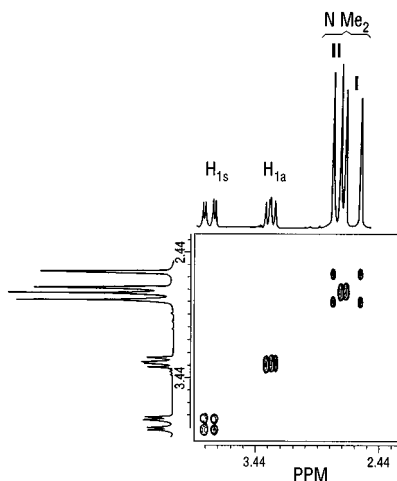


Figure 3. Region of the phase-sensitive 2D ^1H ROESY spectrum of complex **1e**(ClO_4) in 1,1,2,2-tetrachloroethane- d_2 at 28 $^\circ\text{C}$. Only positive NOEs are shown.

protons are clearly indicative of a structure of type **II**. Furthermore, the observed intraligand NOEs are useful for a correct assignment of the ^1H NMR signals. As an example, in the spectrum of **1d** the multiplet centered at 7.05 ppm is assigned to the *meta* protons of the $\text{C}_6\text{H}_4\text{-OMe-4}$ group due to the strong NOE with the methoxy protons, while the singlet at 0.78 ppm is assigned to the $\text{Me}_{(s)}$ protons of the allyl ligand due to its NOE with the central H_2 allylic proton and the singlet at 1.21 ppm is assigned to the $\text{Me}_{(a)}$ protons due to its NOE with the H_{1a} allylic proton.

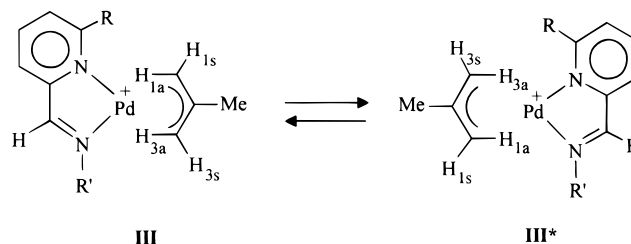
As can be seen in Tables 1 and 2, the isomer distribution depends essentially on the steric requirements of both the allyl and the chelate N-N' ligands. For the more sterically demanding 3-methyl-2-butenyl group the relative abundance of isomer **II** increases with increasing bulkiness of the imino nitrogen substituent R' of the ligand $\text{C}_5\text{H}_4\text{N-2-CH=NR}'$: from 44% for **1a** ($\text{R}' = \text{Me}$) to 79% for **1c** ($\text{R}' = \text{C}_6\text{H}_4\text{OMe-4}$) and finally to 100% for **1b** ($\text{R}' = \text{CMe}_3$). Consistently, when the steric hindrance of the 2-pyridyl group is increased by introducing a methyl substituent on the C(6) ring carbon, the isomer distribution is completely reversed in favor of structure **I**. In fact, the relative abundance of **I** shifts from 21% for **1c** ($\text{R} = \text{H}$, $\text{R}' = \text{C}_6\text{H}_4\text{OMe-4}$) to 100% for **1d** ($\text{R} = \text{Me}$, $\text{R}' = \text{C}_6\text{H}_4\text{OMe-4}$).

For complexes **1a,c**, the isomer distribution appears to be hardly affected by changes in the temperature in the range +10 to -60 $^\circ\text{C}$, suggesting a rather small standard enthalpy value for the equilibrium of isomer interconversion.

For the η^3 -2-butenyl complexes, the *syn* isomers are present in major concentration, and the distribution of isomers **I(s)** and **II(s)** is affected by the steric requirements of the N-N' ligand in the same way as that observed for the isomers **I** and **II** of the η^3 -3-methyl-2-butenyl derivatives: the **II(s)/I(s)** ratio increases with increasing bulkiness of the imino nitrogen substituent R' , whereas the isomer **I(s)** predominates in complex **2d** with the $\text{C}_5\text{H}_4(6\text{-Me})\text{N-2-CH=NC}_6\text{H}_4\text{OMe-4}$ ligand.

The structures of the *anti* isomers **I(a)** and **II(a)** can be assigned only for derivatives **2c,d**, both having $\text{R}' = \text{C}_6\text{H}_4\text{OMe-4}$. The other complexes **2a,b,e** are also present in solution with both isomers **I(a)** and **II(a)**, but an unambiguous assignment based on the previ-

Scheme 2



ously described criterion is not possible in these cases since no significant change in the H(6) chemical shift occurs when the structure is changed from **I(a)** to **II(a)**. Furthermore, the low concentration of the *anti* isomers prevents the observation of some resonances as they are masked by the more intense signals of the *syn* isomers. The total concentration of the *anti* isomers appears to increase with increasing steric demand of N-N' from 8% for **2a** and **2e** to 20 and 22% for **2b** and **2d**, respectively, in line with the observed stabilization of *anti* isomers in the corresponding (η^3 -butenyl)palladium(II) complexes with 1,10-phenanthroline ligands carrying bulky 2,9-substituents.⁹

Isomer Interconversion. The complexes **1a,c,e** or **2a-e** exhibit a dynamic behavior in solution which involves interconversion of isomers **I** \rightleftharpoons **II** for the 3-methyl-2-butenyl derivatives or of isomers **I(s)** \rightleftharpoons **II(s)** and **I(a)** \rightleftharpoons **II(a)** for the 2-butenyl derivatives. This process can be readily monitored by ^1H NMR spectroscopy as it brings about a *syn-syn*, *anti-anti* exchange of the allylic protons and of the allylic methyl substituents in the isomeric pairs. At ambient temperature, no *syn-anti* exchange was detected in chlorinated solvents and even in the more coordinating dimethyl- d_6 sulfoxide, where the rate of *syn-syn*, *anti-anti* exchange is generally so high as to give rise to averaged signals. In the phase-sensitive 2-D ROESY spectrum of **1e** (Figure 3), the absence of positive NOEs (negative cross-peaks) between the *syn* and *anti* protons of isomers **I** and **II** suggests that no *syn-anti* proton exchange takes place, whereas the presence of positive NOEs between the *syn* protons and between the *anti* protons of **I** and **II** clearly demonstrates the occurrence of *syn-syn*, *anti-anti* dynamic exchange.

Similarly, in the allylic methyl region (not shown in Figure 3) the $\text{Me}_{(s)}$ and $\text{Me}_{(a)}$ protons of isomer **I** are in exchange with the $\text{Me}_{(s)}$ and $\text{Me}_{(a)}$ protons of isomer **II**, respectively, whereas no pairwise $\text{Me}_{(s)}\text{-Me}_{(a)}$ exchange is observed. These findings are in agreement with earlier studies on related complexes which showed the *syn-syn*, *anti-anti* exchange (or apparent allyl rotation) to be the dynamic process requiring the lowest activation energy.^{5b}

Formally, a 180° rotation of the η^3 -allyl ligand around its bond axis to the central metal interchanges an isomer of structure **I** into the enantiomeric form of the isomer of structure **II** in Charts 1 and 2 and *vice versa*, with concomitant *syn-syn*, *anti-anti* interchange of allylic protons and methyl groups. Such a process occurs also for the η^3 -2-methyl-2-propenyl complexes **3a-e**. In these cases, the apparent allyl rotation brings about the interconversion of the enantiomeric forms **III** and **III*** of Scheme 2.

(9) Sjögren, M.; Hausson, S.; Norrby, P. O.; Åkermark, B.; Cucciolito, M. L.; Vitagliano, A. *Organometallics* **1992**, *11*, 3954.

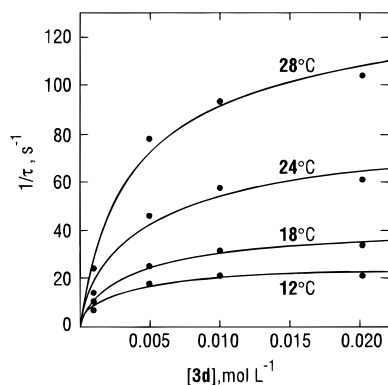


Figure 4. Plot of $1/\tau$ values for the enantiomers of **3d**(ClO₄) vs the total concentration of the complex, at different temperatures in dichloromethane-*d*₂.

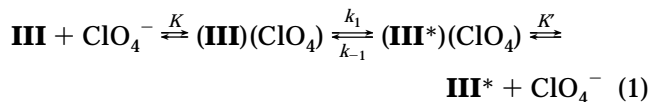
From line shape analysis of variable-temperature ¹H NMR spectra for 0.04 mol L⁻¹ solutions of **3a–e**(ClO₄) in 1,1,2,2-tetrachloroethane-*d*₂ the rates of interconversion were found to depend on the N-N' ligand in the following order: **c** > **d** > **e** > **b** > **a**. For the 2-(iminoethyl)pyridine ligands, both the electronic and steric properties of the imino nitrogen R' substituent are important. The rates decrease considerably when the aryl substituent of **c** (R' = C₆H₄OMe-4) is replaced by the more electron-releasing alkyl groups of **a** and **b** (R' = Me and CMe₃, respectively). For the latter ligands, the rates decrease also when the bulkier CMe₃ substituent is replaced by the methyl group, as can be inferred from the mean lifetime (τ) values of 0.09 and 0.58 s for the enantiomers **III** and **III*** of **3b** and **3a**, respectively, at 60 °C. However, an increase in the steric requirements around the pyridine nitrogen brings about a decrease in the interconversion rates, as it appears from the τ values of 0.021 and 0.082 s for **3c** and **3d**, respectively, at 20 °C.

The rate of the apparent allyl rotation is influenced also by the nature of the allyl ligand. For complexes **1a**, **2a**, and **3a** in 1,1,2,2-tetrachloroethane-*d*₂ solution (0.04 mol L⁻¹), the variable-temperature ¹H NMR spectra afford the following coalescence temperatures: 95 °C for the H_{1a} and H_{3a} protons of **3a** ($\Delta\nu$ = 48 Hz), 28 °C for the α -diimine N-Me protons of the *syn* isomers **I(s)** and **II(s)** of **2a** ($\Delta\nu$ = 45 Hz), and 46 °C for the α -diimine N-Me protons of isomers **I** and **II** of **1a** ($\Delta\nu$ = 52 Hz). No coalescence temperature could be determined for the *anti* isomers **I(a)** and **II(a)** of **2a** because of their low concentration. It thus appears that the rate increases in the order **3a** < **1a** < **2a**, *i.e.* when the η^3 -allyl ligand is changed from 2-methyl-2-propenyl to 3-methyl-2-butenyl and to *syn*-2-butenyl. In general, a marked increase in the rate of apparent allyl rotation is observed on going from the η^3 -2-methyl-2-propenyl to the *syn*- η^3 -2-butenyl complexes of the ligands **a–d**. The dynamic behavior of 2-((dimethylamino)methyl)pyridine derivatives **2e** and **3e** is peculiar since the allyl rotation is slightly faster for **3e** than for the *syn* isomers of **2e**.

As previously reported for **3c**(ClO₄),^{7a} the rate of apparent allyl rotation for the analogous complex **3d**(ClO₄) decreases with decreasing concentration in dichloromethane-*d*₂. Such influence was studied by varying the concentration from 10⁻³ to 2 × 10⁻² mol L⁻¹, at four different temperatures in the range 12–28 °C. Line shape analysis of the ¹H NMR spectra yields the mean

lifetime values (τ) of the interconverting enantiomers **III** \rightleftharpoons **III***, the reciprocals of which depend on the total concentration of the complex **[3d]**, as is shown in Figure 4. Initially, the $1/\tau$ terms increase with increasing concentration and tend to a limiting constant value at higher **[3d]** values.

This behavior may be interpreted on the basis of the associative mechanism 1:



This mechanism involves a fast and reversible association of the cation **III** (or **III***) with the perchlorate anion to form the ion-pair **(III)(ClO₄)** [or **(III*)(ClO₄)**] which undergoes the rate-determining allyl rotation possibly through coordination of ClO₄⁻ in either a sterically nonrigid five-coordinate or in a four-coordinate transient or transition state with a monodentate N-N' ligand.

Ion-pair formation in dichloromethane is well documented.¹⁰ The ionic association equilibria for **3d**(ClO₄) are also supported by electric conductivity measurements at different concentrations. In dichloromethane at 24 °C the molar conductivity values show an initial sharp decrease from 37.6 to 24.3 Ω⁻¹ mol⁻¹ cm² when the concentration is increased from 1 × 10⁻³ to 5 × 10⁻³ mol L⁻¹, followed by a moderate decrease to 21.3 and 19.7 Ω⁻¹ mol⁻¹ cm² when the concentration is further increased to 1 × 10⁻² and 2 × 10⁻² mol L⁻¹, respectively.

Under the reasonable assumption that the enantiomeric species are present as a racemic mixture in an achiral solvent and in association with an achiral anion (**[III]** = **[III*]**, **[(III)ClO₄] = [(III*)(ClO₄)]**) and hence $K = K'$ and $k_1 = k_{-1}$ the exchange rate is given by the expression 2, where **[3d]** is the total concentration of the complex. This equation fits well the experimental

$$\text{rate} = \frac{1}{\tau} [\text{3d}] = \frac{k_1 [\text{3d}] (\sqrt{1/4 + K [\text{3d}]} - 1/2)}{1 + (\sqrt{1/4 + K [\text{3d}]} - 1/2)} \quad (2)$$

rate data of $1/\tau$ vs **[3d]** as is shown by the best-fitting curves of Figure 3. Nonlinear least-square analysis, where k_1 and K are the parameters to be optimized, gives the following values for k_1 (s⁻¹) and K (mol⁻¹ L⁻¹) at the different temperatures:¹¹ 167 ± 20 and 273 ± 105 at 28 °C; 100 ± 14 and 272 ± 128 at 24 °C; 53 ± 4 and 319 ± 76 at 18 °C; 33 ± 4 and 393 ± 198 at 12 °C. The large uncertainties in k_1 and particularly in K values arise from the limited number of the experimental points to be fitted and from the uncertainties in the calculated $1/\tau$ data (5–10%). Owing to the narrow temperature range, a reparametrized model of the Eyring plot was applied to yield the activation parameters $\Delta H^\ddagger = 71.6 \pm 7$ kJ mol⁻¹ and $\Delta S^\ddagger = 35 \pm 7$ J mol⁻¹ K⁻¹.

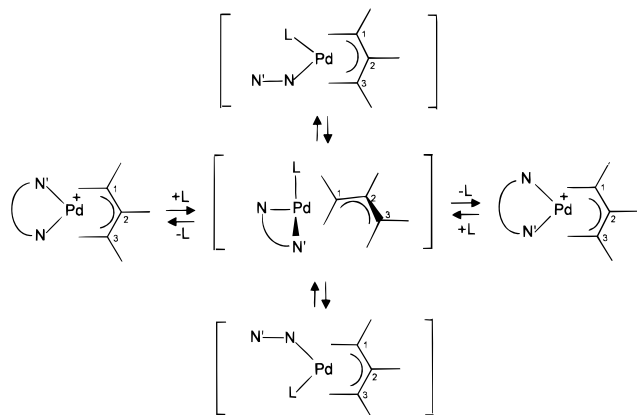
For the complexes [Pd(N-N')(η^3 -2-butenyl)](CF₃CO₂), containing rigid phenanthroline ligands and the moderately coordinating trifluoroacetate anion, activation enthalpies of 48 to 58.2 kJ mol⁻¹ and activation entro-

(10) Reichardt, C. *Solvents and Solvent Effects in Organic Chemistry*; VCH Verlagsgesellschaft: Weinheim, Germany, 1990.

(11) Marquardt, D. W. *SIAM. J. Appl. Math.* **1963**, *11*, 431.

(12) Uguagliati, P.; Michelin, R. A.; Belluco, U.; Ros, R. *J. Organomet. Chem.* **1979**, *169*, 115.

Scheme 3



pies of -10.6 to -50 J mol $^{-1}$ K $^{-1}$ have been reported for 20:1 CD $_2$ Cl $_2$ /CD $_3$ OD solutions.^{5b} The slightly positive ΔS^\ddagger value observed for **3d**(ClO $_4$) (with the poorly coordinating perchlorate anion) may result from an activation process involving either predominant dissociation of a palladium–nitrogen bond or defreezing of solvent molecules from the solvation spheres of the ions in a “loose” ion-pair (**III**)(ClO $_4$) when ClO $_4^-$ enters the palladium coordination sphere. In order to clarify this point, we have examined the temperature and solvent influence on the dynamic behavior of the complex **1e**(ClO $_4$) by reasoning that a possible Pd–NMe $_2$ bond breaking would lead to scrambling of the *N*-methyl groups^{5b,c} due to fast inversion at the uncoordinated sp 3 nitrogen of the 2-((dimethylamino)methyl)pyridine ligand, a process which is known to require a relatively small energy of activation. The phase-sensitive 2-D 1 H ROESY spectrum of **1e**(ClO $_4$) in 1,1,2,2-tetrachloroethane- d_2 at 28 °C (Figure 3) shows that the NMe $_2$ protons of isomer **I** (at 2.72 and 2.59 ppm) are in mutual exchange with the NMe $_2$ protons of isomer **II** (at 2.82 and 2.76 ppm), whereas no intramolecular exchange of the NMe $_2$ protons within each isomer is observed. However, upon heating of the solution to 90 °C, the four NMe $_2$ signals of isomer **I** and **II** coalesce into a single resonance at 2.80 ppm. A similar type of coalescence of the NMe $_2$ signals into a rather broad absorption at 2.83 ppm is also detected in the 1 H NMR spectrum of **1e**(ClO $_4$) in dimethyl- d_6 sulfoxide at 28 °C. From these observations it appears that in 1,1,2,2-tetrachloroethane- d_2 the **I** \rightleftharpoons **II** interconversion does not involve Pd–NMe $_2$ bond breaking at any appreciable rate at 28 °C, whereas this takes place either when the temperature is raised to 90 °C or when **1e**(ClO $_4$) is dissolved in the more coordinating dimethyl- d_6 sulfoxide at 28 °C. In other words, a much higher energy is required for the rupture of the Pd–NMe $_2$ bond to occur during the apparent allyl rotation in this system.

On the basis of the above results, the activation process for the isomer interconversion may be described as in Scheme 3. The four-coordinate species with monodentate N–N' ligands are likely to be involved as short-lived intermediates in the exchange between free and coordinated N–N' ligands which takes place in the mixtures [Pd(η^3 -allyl)(N–N')] $^+$ /N–N'.^{5b,7a,b}

On the other hand, the observed influence of concentration, solvent, and allyl methyl substituents on the dynamic behavior of the cationic complexes under study can hardly be explained by a dissociative mechanism

Table 4. Elemental Analysis Data (%)^a

complex	C	H	N
1a (ClO $_4$)	36.6 (36.47)	4.3 (4.34)	7.1 (7.09)
1b (ClO $_4$)	41.3 (41.21)	5.3 (5.30)	6.4 (6.41)
1c (ClO $_4$)	44.4 (44.37)	4.3 (4.35)	5.8 (5.75)
1d (ClO $_4$)	45.7 (45.53)	4.5 (4.62)	5.6 (5.59)
1e (ClO $_4$)	37.9 (37.97)	5.1 (5.15)	6.7 (6.81)
2a (ClO $_4$)	34.5 (34.67)	3.9 (3.97)	7.3 (7.35)
2b (ClO $_4$)	39.8 (39.73)	5.1 (5.00)	6.5 (6.62)
2c (ClO $_4$)	43.2 (43.15)	4.1 (4.05)	5.8 (5.92)
2d (ClO $_4$)	44.5 (44.37)	4.2 (4.35)	5.7 (5.75)
2e (ClO $_4$)	36.4 (36.28)	4.7 (4.82)	7.0 (7.06)
3b (ClO $_4$)	39.7 (39.73)	4.9 (5.00)	6.6 (6.62)
3d (ClO $_4$)	44.4 (44.37)	4.3 (4.35)	5.7 (5.75)
3e (ClO $_4$)	36.4 (36.28)	4.9 (4.82)	7.0 (7.06)

^a Calculated values in parentheses.

involving a spontaneous, nonassisted Pd–N bond breaking as the rate-determining step, such as that proposed for [Pd(η^3 -allyl)(bpm)] $^+$.^{7c} For a unimolecular activation process yielding a three-coordinate intermediate, changes in complex concentration or in the nature of the solvent would be expected to have little, if any, influence on the rate of allyl rotation. Stabilization of the three-coordinate intermediates by coordination of the counteranion and/or of the solvent would also have no accelerating effect if this occurs in a subsequent fast step.

The observed increase in the allyl rotation rate on going from **3a** to **2a** might well be explained by a greater steric strain in the η^3 -2-butenyl complex **2a**, arising from interaction of the allyl methyl group with the *N*-substituents of the ligand **a**, which would lower the activation energy for the Pd–N bond breaking. If this would be the case, however, an even greater rate should be observed for complex **1a** containing the more sterically demanding η^3 -3-methyl-2-butenyl ligand. In contrast, the rate decreases on going from **2a** to **1a**.

In the proposed associative mechanism, the steric influence of the N–N' and the η^3 -allyl ligands is interpreted in terms of an interplay of steric factors in the stabilization of the four-coordinate complexes and in the ease of rearrangement of the five-coordinate transients in the sense that an increasing ligand bulkiness would destabilize the four-coordinate [Pd(η^3 -allyl)N–N'] $^+$ compound^{5b} but, at the same time, would hinder the ligand site changes in the five-coordinate species.

The higher interconversion rates for the cations **3c,d** (both with R' = C $_6$ H $_4$ OMe-4) relative to **3a,b** (with the more electron-releasing imino nitrogen substituents R' = Me and CMe $_3$, respectively) may be related to a greater positive charge on the central metal, which makes easier the formation of five-coordinate species with the incoming nucleophile L (Scheme 3).

Experimental Section

Physical Measurements. 1 H NMR spectra were recorded on a Bruker AM400 instrument, operating at 400.13 MHz. Spectra have been typically obtained with 128 transients over a sweep width of 13 ppm with a relaxation delay of 3 s each scan. A pulse corresponding to 60° was applied. The samples were prepared by dissolving 0.02 mmol of the complex in 0.5 mL of deuterated solvent. 1 H NMR chemical shifts are given in δ (ppm) relative to Me $_4$ Si as the internal standard. The temperature was calibrated using a separate methanol sample. 1 H 2D ROESY spectra have been obtained in the phase-

Table 5. ^1H NMR Data for the Complexes $[\text{Pd}(\eta^3\text{-2-MeC}_3\text{H}_4)(\text{N-N}')]\text{ClO}_4$

complex	allyl protons			N-N' protons			other signals
	H_{syn}	H_{anti}	Me	N=CH	H(6)	Me(6)	
3b ^a	4.13 d, 4.09 d (2.1) ^b	3.44 s, 3.16 s	2.19 s	8.60 s	8.78 m		1.44 s [CMe ₃]
3d ^a	4.24 s, 3.64 s	3.42 s, 3.21 s	2.08 s	8.65 s		2.72 s	
3e ^c	3.75 s, 3.69 s	3.09 s	2.17 s		8.51 m		2.88 s, 2.81 s [NMe ₂]

^a In dichloromethane-*d*₂ at -60 °C. ^b Long-range $\text{H}_{\text{syn}}\text{-H}_{\text{syn}}$ coupling constant. ^c In 1,1,2,2-tetrachloroethane-*d*₂ at 28 °C.

sensitive mode using the TPPI phase cycle¹³ with the ROESY pulse sequence,¹⁴ modified to eliminate the offset dependence of cross-peak intensity.¹⁵ A total of 128 transients on a size of 2K were accumulated in the phase-sensitive mode for 512 experiments. A spinlock period corresponding to a transverse mixing time of 0.3 s was applied. Data were processed with the 2D NMR program TRITON, written by Boelens and Vuister and licensed by the University of Utrecht, Utrecht, The Netherlands (courtesy of Prof. R. Kaptein). Elaboration of spectra was carried out on a Digital Graphic workstation. A sine bell apodization function, shifted by $\pi/3$, was applied in both dimensions. A zero filling was applied in *f1* in order to obtain a real $1\text{K} \times 1\text{K}$ matrix.

The electric conductivity was measured with a CDM83 conductivity meter. The IR spectra of solid samples were recorded in the range 4000–200 cm^{-1} on a Perkin-Elmer 983 G instrument using Nujol nulls and CsI windows.

Materials. The 2-(iminomethyl)pyridines¹⁶ and 2-((dimethylamino)methyl)pyridine¹⁷ were prepared by published methods. The dimers $[\text{Pd}(\mu\text{-Cl})(\eta^3\text{-allyl})]_2$ (allyl = 1-MeC₃H₄, 2-MeC₃H₄, 1,1-Me₂C₃H₃) were prepared according to the literature.¹⁸ All other chemicals were commercial grade and were purified or dried by standard methods, when required.¹⁹ All the complexes $[\text{Pd}(\eta^3\text{-allyl})(\text{N-N}')]\text{ClO}_4$ were prepared by

(13) Marion, D.; Wüthrich, K. *Biochem. Biophys. Res. Commun.* **1983**, *113*, 964.

(14) Bothner-By, A. A.; Stephens, R. L.; Lee, J.; Warren, C. D.; Jeanloz, R. W. *J. Am. Chem. Soc.* **1984**, *106*, 811.

(15) Griesinger, C.; Ernst, R. R. *J. Magn. Reson.* **1987**, *75*, 261.

(16) Matsubayashi, G.; Okumaka, M.; Tanaka, T. *J. Organomet. Chem.* **1974**, *66*, 465.

(17) Erdtman, H.; Haglid, F.; Wellings, I. *Acta Chem. Scand.* **1963**, *17*, 1726. Fischer, A.; King, M. J.; Robinson, F. P. *Can. J. Chem.* **1978**, *56*, 3059.

(18) Powell, J.; Shaw, B. L. *J. Chem. Soc. A*, **1967**, 1839. Numata, S.; Okawara, R.; Kurosawa, H. *Inorg. Chem.* **1977**, *16*, 1737. Dent, W. T.; Long, R.; Wilkinson, A. J. *J. Chem. Soc.* **1964**, 1585. Ashraf, M. C.; Burrowes, T. G.; Jackson, W. R. *Aust. J. Chem.* **1976**, *29*, 1111.

(19) Armarego, W. L. F.; Perrin, D. D. *Purification of Laboratory Chemicals*, 3rd ed.; Pergamon Press: New York, 1988.

the same procedure previously described for **3a**(ClO₄).^{7a} The products were reprecipitated three times from a CH₂Cl₂/Et₂O solvent mixture in order to eliminate any trace of impurities, such as Cl⁻ and/or uncoordinated α -diimine, which can accelerate the dynamic behavior in solution. Because of the straightforward method of preparation, the cationic complexes can be completely characterized by their ^1H NMR spectral data. However, elemental analysis, IR spectra in the solid state, and molar conductivity measurements were also carried out in order to ascertain the composition, the presence of the ClO₄⁻ anion [$\nu(\text{Cl-O})$ around 1100 cm^{-1} and $\delta(\text{Cl-O})$ in the range 630–620 cm^{-1}], and the nature of uni-univalent electrolytes (molar conductivity in the range 114–99 $\Omega^{-1} \text{cm}^2 \text{mol}^{-1}$ for $1 \times 10^{-3} \text{mol L}^{-1}$ MeOH solutions at 25 °C). The elemental analysis data of the studied complexes and the ^1H NMR data of the η^3 -2-methyl-2-propenyl complexes are given in the Tables 4 and 5.

The organometallic perchlorate salts were handled in a hood with a protecting screen as to reduce the potential hazard of explosion.

Line Shape Analysis. The evaluation of lifetimes in the exchange dynamics was obtained by fitting the experimental points of the enlarged region of interest in the ^1H NMR spectra by a total line shape analysis. The equally populated two-site exchange algorithm²⁰ was applied and fitted by a nonlinear regression routine contained on the program Kaleidograph for a Macintosh Power PC. A mean residual error less than 0.01% was considered as acceptable.

Acknowledgment. Financial support by the Italian Ministero per l'Università e la Ricerca Scientifica e Tecnologica (Research Fund 40%) is gratefully acknowledged. The technical support of Fabio Bertocchi in running the NMR spectra and the maintenance of the NMR equipment is gratefully acknowledged.

OM9608420

(20) Gutowsky, H. S.; Holm, C. H. *J. Chem. Phys.* **1956**, *25*, 1228.